

GT2011-46\* \* (

## OPTIMIZATION OF A 3-STAGE BOOSTER- PART 2: THE PARAMETRIC 3D BLADE GEOMETRY MODELING TOOL

Kiran Siddappaji \*  
Mark G. Turner  
Soumitr Dey  
Kevin Park

Department of Aerospace Engineering  
University of Cincinnati  
Cincinnati, OH, USA

Ali Merchant  
CADNexus  
Burlington, MA, USA

### ABSTRACT

*A parametric approach for blade geometry design has been developed to obtain 3D blade models. The geometry of the blade is defined by a basic set of parameters that are first obtained from an axisymmetric solver. These parameters include the leading edge meridional coordinates, flow angles, axial chord, and the meridional coordinates of streamlines. Other parameters such as thickness to chord ratio need to be defined. Using these parameters the 2D airfoils are created and are stacked radially using one of the many multiple options that define the stacking axes from several additional parameters. The tool produces the desired number of 2D sections in a normalized coordinate system. Each blade section is then transformed to a 3D Cartesian coordinate system. Using Unigraphics-NX (CAD package), these sections are lofted and a 3D blade model is obtained. Parametric update of the spline points defining the 3D blade sections results in new blade shapes without going directly back into the CAD system. The importing of the geometry into a CFD solver, and a finite element solver to determine mode shapes and stresses is demonstrated. Full details of the blade procedure is presented for a 3-Stage Booster design. This parametric approach for defining blade geometry and how it lays a groundwork for a high-fidelity optimization procedure is described.*

### NOMENCLATURE

a Offset value

b Intermediate extruded blade scale factor  
i Incidence angle  
L Reference length  
m Meridional coordinate  
np Number of points  
nspn Number of streamlines  
r Radial coordinate  
V Absolute flow velocity  
x Axial coordinate

### Greek

$\alpha$  Absolute flow angle  
 $\beta$  Relative flow angle  
 $\delta$  Deviation angle  
 $\zeta$  Stagger angle  
 $\theta$  Tangential direction  
 $\phi$  Angle defined as  $\arctan(V_r/V_x)$   
 $\bar{\omega}$  Loss coefficient

### Subscripts

b Blade  
r Radial  
ref Reference  
x Axial  
s Streamline  
LE Leading Edge  
TE Trailing Edge  
3D Three dimensional

\*Address all correspondence to this author. Email: s2kn@mail.uc.edu

## Abbreviations

CAD	Computer Aided Design
CFD	Computational Fluid Dynamics
EEE	Energy Efficient Engine
FEA	Finite Element Analysis
UG	UniGraphics-NX
2D	Two Dimensional
3D	Three Dimensional

## INTRODUCTION

The blade geometry design process plays an important role in the development of any turbomachinery design system. A parametric approach for the geometry design is essential as the process is iterative in nature and helps in maintaining the blade topology.

There are several papers on a parametric approach to the blade geometry and its linkage to an optimization process. One paper by Gräsel et al. [1] describes a complete parametric model for the blade design where the blades are free form shapes defined by Spline-functions. It also describes modification of aerofoils with the help of the curvature distribution defined by control points. Interaction with a CAD interface and how the parameters are optimized is also discussed. Another paper by Dutta et al. [2] describes an automated process of a non-dimensional quasi-3D blade design with parameterization of the camber-line angle and thickness distributions and blade inlet and outlet angles. It talks about an optimization loop including geometry generation, certain blade-to-blade computations and post-processing, and how each parametric variable has an impact on the optimizer. A complete framework for multidisciplinary design optimization with multi-objective functions and multi-fidelity has been explained in detail in the paper by Turner et al. [3]. It also talks about the consistency of the geometry at medium and high fidelity.

This paper represents part 2 of the optimization of a 3-stage booster. Part 1 of the paper describes the interface for the optimizer and explains the multi-disciplinary optimization approach to axisymmetric compressor design. A parametric tool for generating 3D blade geometry is presented in detail in this paper. A 3-Stage Booster design is used as an example to show the capability of this tool. Newer blade geometry shapes are obtained by parametric update of the spline points defining the blade shape without any CAD interference hence avoiding CAD model translation errors. It also deals with the process of performing a high fidelity 3D-CFD analysis on the designed blade with proper boundary conditions. The CFD analysis is useful in determining the aerodynamic performance of the designed blade and acts as a feedback in modifying the design to obtain desired working parameters. This paper also discusses a finite element analysis of the blade by determining the stresses and the modal shapes thereby investigating the structural integrity of the design. A similar finite element analysis is done for a disk generated using *Unigraphics-NX* in order to obtain a complete understanding of the stresses acting upon both the disk and the blade models. The next stage is the optimization of the parameters which define the blade geometry. This paper shows all the parts needed for high fidelity optimization and provides a starting point for the high

fidelity optimization with single or multi-objective functions.

## 3D BLADE GENERATOR MODEL DEVELOPMENT

This section deals with the development of the blade generator model explaining how the input parameters are utilized in creating blade sections and performing mathematical operations to finally obtain a 3D blade model. Figure 1 explains the process flow involved. Details have been included in this discussion because they are important to achieve smooth blades for which the parameterization is robust.

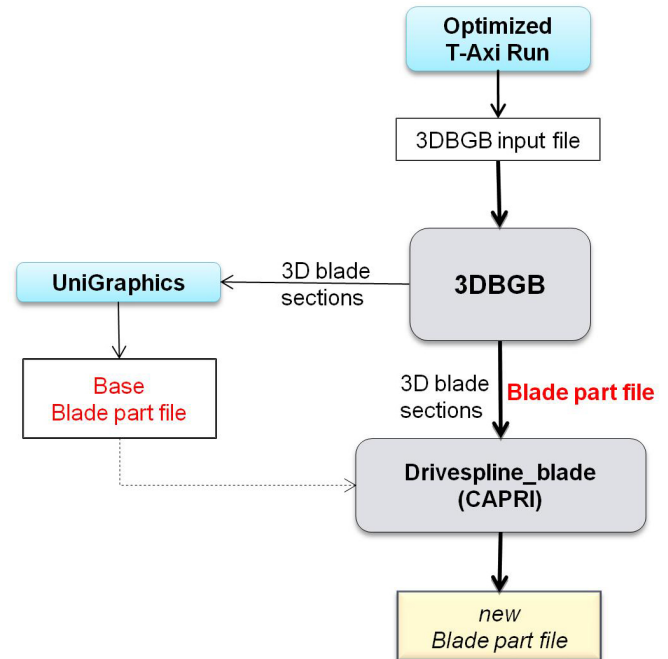


Figure 1. 3D Blade Design process Flowchart.

## Input File

The input file for the 3DBGB (3 Dimensional Blade Geometry Builder) code contains parameters defining the blade geometry required to build a 3D blade. The parameters are defined at each streamline passing through the blade as below:

1.  $x, r$  coordinates of the Leading and Trailing Edge of the blade.
2. flow angles at inlet and outlet of the blade.
3. relative inlet mach number.
4. thickness to chord ratio.
5. axial chord values.
6. incidence and deviation angles.

It contains stacking options and control points defining meridional and theta offset. The file also contains the  $m'_s, x_s$  and  $r_s$  coordinates for all the  $nspn$  streamlines defined from an axisymmetric run like T-Axi [4–7], or smooth lines between the hub and casing.

## Blade section construction

A blade is made up of a specific number of blade sections as shown in Figure 2. A blade section comprises a suction side curve and a pressure side curve built around a mean camber curve which passes through the leading edge and the trailing edge of the blade section as shown in Figure 3. Also, in Figure 3, blade

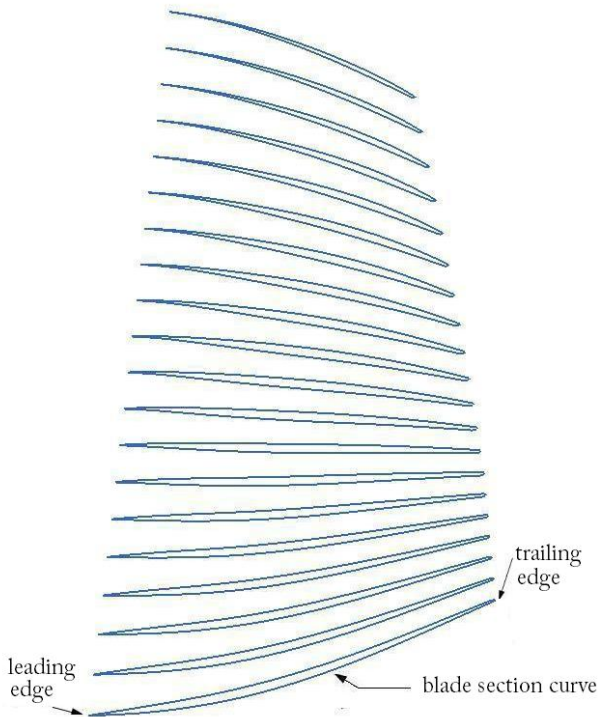


Figure 2. A blade showing the blade sections.

metal angle at inlet is defined by  $\beta_{in}^*$  and at the exit is defined by  $\beta_{out}^*$  and the flow angles at inlet and exit are  $\beta_{in}$  and  $\beta_{out}$  respectively. The incidence angle  $i$  and the deviation angle  $\delta$  are given as below:

1. *Incidence Angle,  $i$* : If  $\beta_{in}^*$  greater than zero then  $i = \beta_{in} - \beta_{in}^*$  and if  $\beta_{in}^*$  is less than zero then  $i = \beta_{in}^* - \beta_{in}$ .
2. *Deviation Angle,  $\delta$* : If camber is negative then  $\delta = \beta_{out} - \beta_{out}^*$  and if camber is positive then  $\delta = \beta_{out}^* - \beta_{out}$ .

Figure 4 shows the blade section rotated by the stagger angle,  $\zeta$  and placed on the chord.

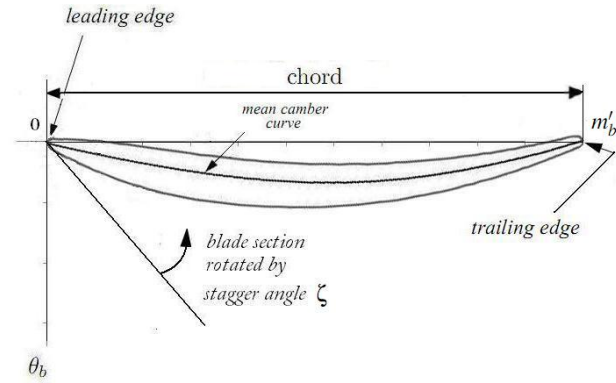


Figure 4. Blade section on the normalized chord.

The mean camber line is built using the flow angles ( $\beta_{in}, \beta_{out}$ ), thickness to chord ratio and the axial chord value. The camber line definition used is a mixed camber line which is partly cubic in nature. The analytical form of the camber line normalized displacement,  $cam$  is expressed in Eq.(7) and  $u$  is the non-dimensional chord (100 points usually used) defining the curve.

1. In Eq.(7)  $aa, bb, cc, dd$  are the coefficients of the cubic equation and  $ub$  is the varying parameter which defines the camber line.
2.  $s_1, s_2$  are the slopes at inlet and exit of the blade section.
3.  $fl_1$  = constant slope at inlet as seen in Figure 6.
4.  $fl_2$  = constant slope at exit as seen in Figure 6.
5.  $c_1, c_2$  are the derivatives of  $u_1, u_2$  with respect to angle where  $u_1, u_2$  are defined as given below.

$$s_1 = \tan \beta_{in} \quad (1)$$

$$s_2 = \tan \beta_{out} \quad (2)$$

$$u_1 = fl_1 \cos \beta_{in} \quad (3)$$

$$c_1 = fl_1 \sin \beta_{in} \quad (4)$$

$$u_2 = 1 - fl_2 \cos \beta_{out} \quad (5)$$

$$c_2 = -fl_2 \sin \beta_{out} \quad (6)$$

$$cam = aa(ub)^3 + bb(ub)^2 + cc(ub) + dd \quad (7)$$

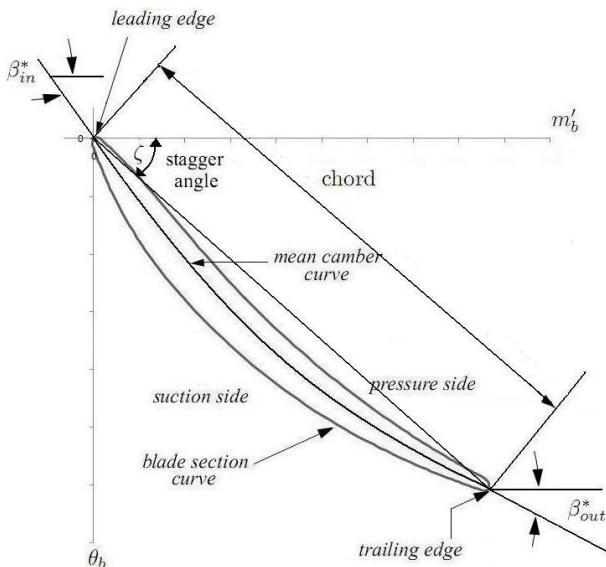


Figure 3. Blade section on the mean camber curve.

$$ub = u - u_1 \quad (8)$$

$$dd = c_1 \quad (9)$$

$$cc = s_1 \quad (10)$$

$$aa = \frac{s_1 + s_2 - 2\left(\frac{c_2 - dd}{xb}\right)}{(xb)^2} \quad (11)$$

$$bb = \frac{-s_1(xb) - aa(xb)^3 + c_2 - dd}{(xb)^2} \quad (12)$$

$$xb = u_2 - u_1 \quad (13)$$

A plot showing the camber line defined by the 100 points is shown in Figure 5 and Figure 6 shows the camber plot of 10th and 11th blade sections for rotor 1 blade of the re-engineered GE EEE high pressure compressor. Also, the curvature of the camber line for the 10th and 11th blade sections are plotted as shown in Figure 7. All these plots are with respect to  $u$ , the non-dimensional chord (100 points usually used) defining the curve.

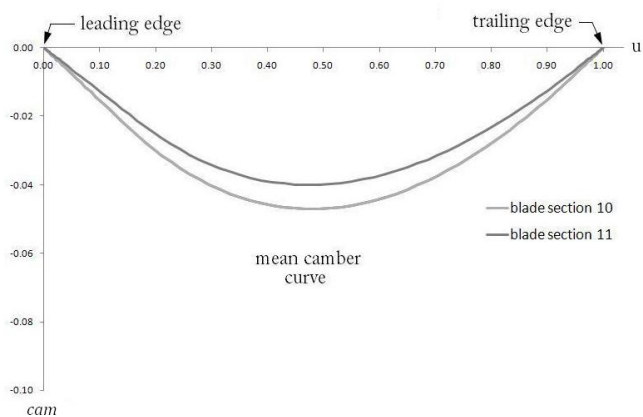


Figure 5. Camber line plot of blade sections 10 and 11 of the GE EEE HPC rotor 1 blade.

An elliptical Leading Edge and circular Trailing Edge are used to get the desired blade section curve. The 2D airfoil thus obtained, contains  $np$  values of  $m'_b, \theta_b$  coordinates in the meridional coordinate system. The coordinates are generated in such a manner that the leading edge value starts at the origin for each blade section.

### Governing Equations

The coordinate system used is shown in Figure 8. The meridional view of the streamlines with the leading edge and the trailing edge is shown in Figure 9. The 3D blade is constructed using the following mathematical approach:

1. streamline coordinates:  $m'_s, x_s, r_s$ .
2. airfoil coordinates:  $m'_b, \theta_b$ .

The projection of the streamline onto the meridional plane  $x - r$  is given by:

$$dm_s = \sqrt{(dr_s)^2 + (dx_s)^2} \quad (14)$$

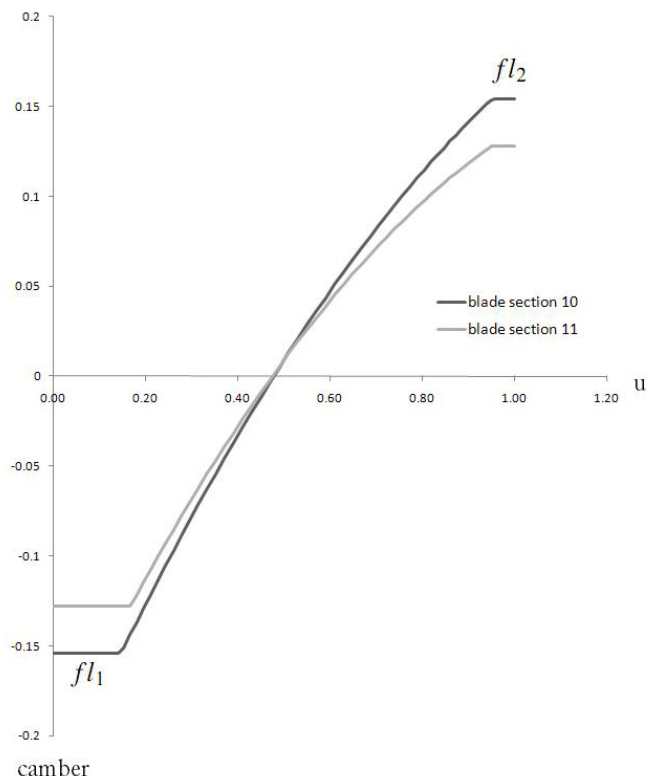


Figure 6. Camber plot of blade sections 10 and 11 of the GE EEE HPC rotor 1 blade.

The normalized differential arc length is defined by:

$$dm'_s = \frac{dm_s}{r_s} \quad (15)$$

The  $m'_s$  coordinate of the streamline is obtained by:

$$m'_s = \int \frac{dm_s}{r_s} = \int \frac{\sqrt{(dr_s)^2 + (dx_s)^2}}{r_s} \quad (16)$$

If the airfoil is designed on constant radius sections, then

$$m'_s = \int \frac{dx_s}{r_s} \quad (17)$$

which represents a normalized axial coordinate.

### Offset between streamline and blade meridional coordinates

The streamline definition extends to both upstream of the leading edge to downstream of the trailing edge of the blade. This is done in order to give provision for a robust mapping. The streamline coordinates  $x_s, r_s$  are splined using a cubic spline with  $m'_s$  as the spline parameter. The leading edge  $m'_s$  value,  $m'_{sLE}$  is calculated on each of the streamline by taking the inverse spline of  $x(m'_s)$  evaluated at  $x_{LE}$  as shown in Figure 10.

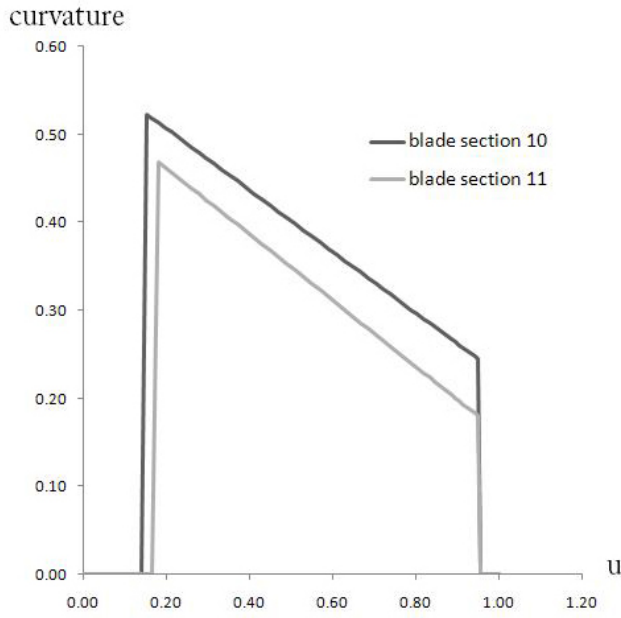


Figure 7. Plot showing the curvature of the camber line of blade sections 10 and 11 of the GE EEE HPC rotor 1 blade.

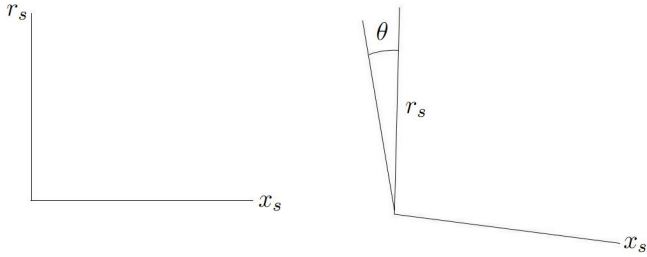


Figure 8.  $r - x - \theta$  space for the 3D blade.

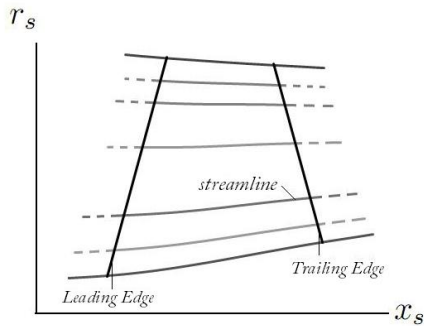


Figure 9. Meridional view of the blade.

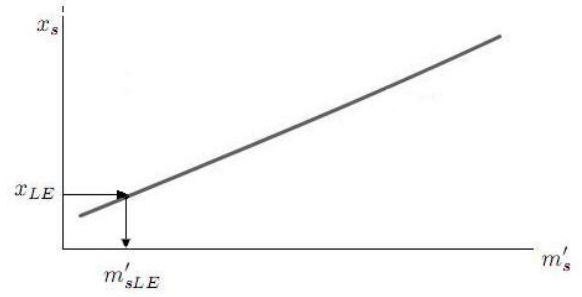


Figure 10.  $m'_{sLE}$  obtained using inverse spline on  $m'_s$ .

There exists an offset between the blade leading edge  $m'_{bLE}$  and the streamline leading edge  $m'_{sLE}$ . This is because the zero  $m'_s$  on each streamline is different from the  $m'_{bLE}$  on each blade section corresponding to the streamline. The offset is expressed as:

$$\delta m' = m'_{sLE} - m'_{bLE} \quad (18)$$

This offset is necessary to make each blade section conform on the corresponding streamline precisely. Similarly, there is an offset added to the  $\theta_b$  coordinates.

$$\theta_{3D} = \theta_b + \delta\theta \quad (19)$$

### Streamwise Coordinates Calculation

Once the offset is calculated for each section the streamwise meridional coordinate  $m'_{3D}$  for each blade section is obtained by adding the offset to the blade meridional coordinates  $m'_b$  of each blade section.

$$m'_{3D} = m'_b + \delta m' \quad (20)$$

The streamwise  $x_{3D}$  and  $r_{3D}$  coordinates are calculated by evaluating the spline at every streamwise meridional coordinate such that all the  $m'_{3D}$  values have corresponding  $x_{3D}$  and  $r_{3D}$  values as shown in the Figure 11 and Figure 12. The splined values of streamline  $x_s$  and  $r_s$  coordinates are used in the spline interpolation.

1.  $x_{3D}$  = spline evaluated at each  $m'_{3D}$  for all the  $np$  points of each blade section.
2.  $r_{3D}$  = spline evaluated at each  $m'_{3D}$  for all the  $np$  points of each blade section.

Hence we have the  $x_{3D}$ ,  $r_{3D}$  and  $\theta_{3D}$  values for all the  $nspn$  blade sections in the cylindrical coordinate system.

### Coordinate Transformation

The normal practice is to obtain a 3D blade in the cartesian coordinate system as most of the CAD packages exist in this system. Therefore a coordinate transformation from the cylindrical

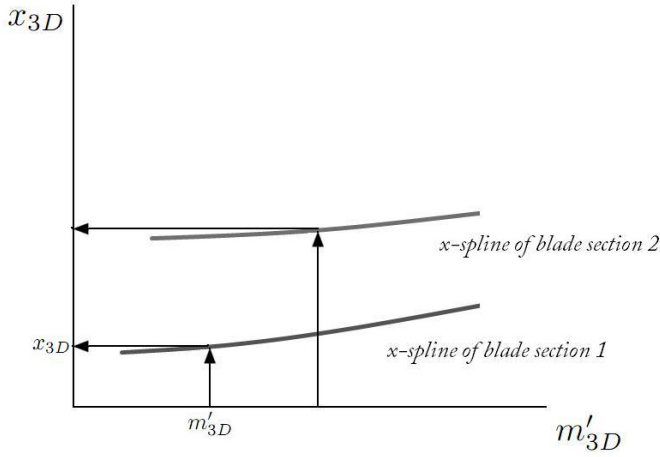


Figure 11.  $x_{3D}$  obtained by spline evaluation at each  $m'_{3D}$  of each blade section.

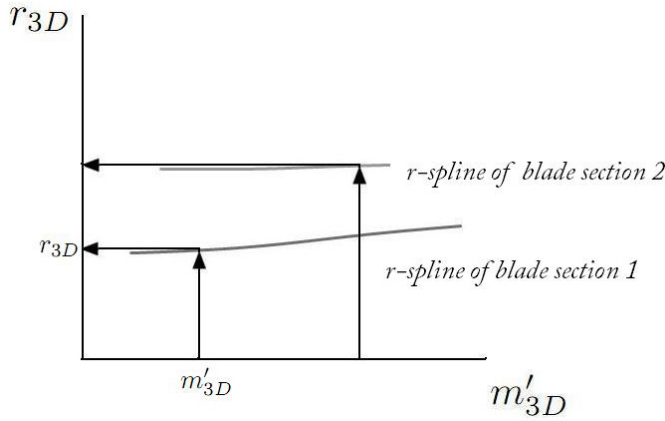


Figure 12.  $r_{3D}$  obtained by spline evaluation at each  $m'_{3D}$  of each blade section.

system to the cartesian system is necessary. The engine axis is assumed to be along the X-axis which makes the  $x$ -values remain the same in both coordinate systems. The transformation is as follows:

$$x_{3D} = x_{3D} \quad (21)$$

$$y_{3D} = r_{3D} \times \sin \theta_{3D} \quad (22)$$

$$z_{3D} = r_{3D} \times \cos \theta_{3D} \quad (23)$$

### 3D Blade Stacking

At this stage all the 3D coordinates of the  $n_{spn}$  blade sections are present in the cartesian system. These sections are stacked using a stacking axis. There can be many options of stacking. One option is where the sections are stacked with

their leading edge ( $x_{LE}$  values in the axisymmetric view) as the stacking axis and taking  $\theta_{LE}$  as zero.

It also can have a stacking axis option defined as a B-spline curve with very few control points. One such case is where the leading edge B-spline curve is defined by a very few control points ( $span, \delta m'$ ). The normalized spanwise location for each streamline is obtained as below.

A straight line with constant  $x$  ( $x_{LE}$  value at the hub) is created which intersects all the streamlines. The  $m'_{xc}$  values for the intersection points on the streamline is obtained by taking the inverse spline of  $xc$  ( $x_{LE}$  value at the hub) on each streamline. Once we have the  $m'_{xc}$  values, the  $r_{xc}$  values at each streamline is obtained by the spline interpolation method explained previously. Once all the  $r_{xc}$  values are evaluated, the reference length is calculated by subtracting the  $r_{xc}$  value at the tip streamline from  $r_{xc}$  value at the hub streamline. The normalized span of  $n^{th}$  streamline is given by

$$span(n) = r_{xc}(n) - r_{xcHUB} \quad (24)$$

$$\widetilde{span}(n) = span(n)/(L_{ref}) \quad (25)$$

At these span points, the corresponding  $\delta m'$  values at each streamline are evaluated from the  $\delta m'$  curve obtained by the control points. This is done by finding the intersection points of a line passing through the span points on the  $\delta m'$  curve at each streamline.

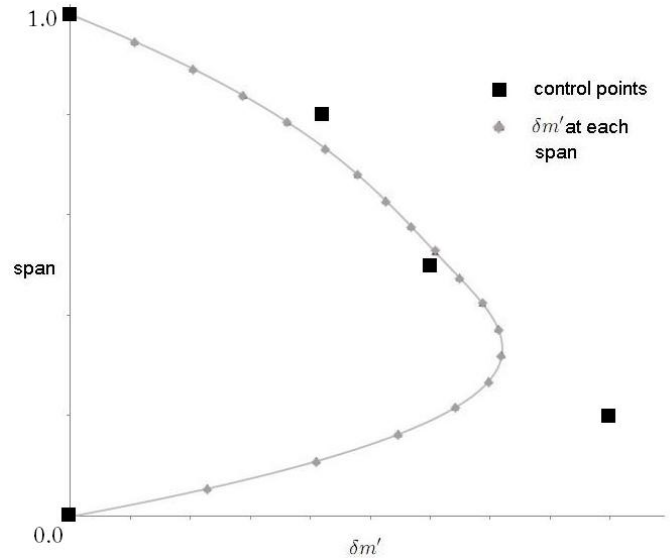


Figure 13.  $\delta m'$  evaluated at each span.

The streamwise meridional coordinates for each blade section for this case will be

$$m'_{3D} = m'_b + \delta m' + m'_{xc} \quad (26)$$

Figure 13 shows the  $\delta m'$  evaluated at each span for all the streamlines on the  $\delta m'$  curve defined by the control points. Similarly, the tangential lean of the blade can be modified by calculating the theta offset from a  $\delta\theta$  curve defined by few control points (span,  $\delta\theta$ ) and the streamwise theta coordinates for each blade section will be

$$\theta_{3D} = \theta_b + \delta\theta \quad (27)$$

Finally, using the coordinate transformation the 3D blade coordinates in the cartesian system is obtained for this case.

### Output files

The blade generator code outputs *nspn* data files which contain *np* values of 3D coordinates for all the *nspn* blade sections. The number of coordinates in the 3D blade sections are kept the same as the number of coordinates in the 2D airfoil sections. The 3D blade section files can act as input files for any CAD package to obtain a 3D Blade CAD model.

### 3D Blade CAD Model

All the data files are imported in Unigraphics (CAD package) where the 3D blade is obtained by stacking all the *nspn* 3D blade sections. Then, lofting is performed by meshing the blade sections to get a smooth 3D blade as shown in the Figure 14.

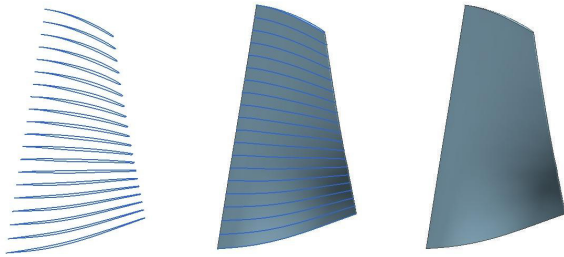


Figure 14. 3D Blade lofted in UG.

### Connecting with CAPRI

CAPRI stands for *Computational Analysis PRogramming Interface*. The 3D Blade constructed in UG is a base model and using CAPRI [8, 9], newer blade shapes are obtained by simply updating the spline information of each 3D blade section on the base model. A simple script written in C integrates the 3D blade part file and the CAPRI interface through which the spline update is done and hence the blade geometry is morphed parametrically. The advantage of using CAPRI is that the geometry data remains in the CAD system and avoids the geometry translation errors during morphing of the blade geometry.

Writing Ufunc (the native UG programming language) routines make sense for a one-off function. Even then it is not trivial to code, debug, and productize new functionality in the short span of time allotted in typical research projects.

Putting together a complete software design suite requires proper architecture, data model, robustness in behavior, just like any other commercial development platform. This is what CAPRI offers for building a multi-disciplinary design suite. It is a stable commercial product that saves significant time and effort in development, deployment, and maintenance of multi-disciplinary design suites that need to interface with CAD. It does not require low-level expertise in CAD or CAD programming to use, and provides an intuitive engineering interface to CAD for MDAO applications. Developing Ufuncs in place of CAPRI could have been done, but with more time and effort.

### Extruded Blade

An extruded blade is often needed by grid generators because of tolerance issue. It also becomes a useful feature. It can be obtained through the code by a simple offset of the hub and the tip streamline coordinates in the normal direction to the streamline. The offset value used here is 0.1 percent of the reference length. At any point  $m'_s$ , the normal in the x-direction,  $x_{NORM}$  and the normal in the r-direction,  $r_{NORM}$  are calculated by using the orthogonal property between the normal and the slope at that point.

$$x_{NORM} = \frac{dr_s}{dm'_s} \quad (28)$$

$$r_{NORM} = -\frac{dx_s}{dm'_s} \quad (29)$$

So, the offset in the normal direction is given by

$$\Delta n = aL_{ref}, \quad (30)$$

where  $a$  is 0.001 and  $L_{ref}$  is unity. Also,

$$\Delta n = b\sqrt{x_{NORM}^2 + r_{NORM}^2} \quad (31)$$

where  $b$  is an intermediate extruded blade scale factor.  $b$  is solved

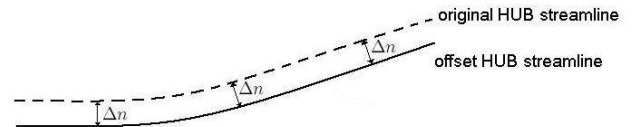


Figure 15. Offset at the hub streamline.

using the 2 equations above, and the offset at the hub is obtained:

1. streamline coordinates at the hub :  $x_{sHUB}, r_{sHUB}$
2. streamline coordinates at the tip :  $x_{sTIP}, r_{sTIP}$

$$x_{sExtruded} = x_{sHUB} + (b \times x_{NORM}) \quad (32)$$

$$r_{sExtruded} = r_{sHUB} + (b \times r_{NORM}) \quad (33)$$

and the offset at the tip as

$$x_{sExtruded} = x_{sTIP} - (b \times x_{NORM}) \quad (34)$$

$$r_{sExtruded} = r_{sTIP} - (b \times r_{NORM}) \quad (35)$$

The original hub and tip streamline coordinates are replaced by the extruded hub and tip streamline coordinates in the input file and the blade section parameters of the original hub and tip streamlines are used. The blade generation process is the same as explained above with a resulting extruded 3D blade.

## CFD ANALYSIS

FINE/Turbo v8 by Numeca [10] was used for a 3D CFD analysis on the blade CAD model obtained. FINE/Turbo is a high fidelity package which has its own gridding tool, solver and a post processor.

### Gridding

The 3D blade section geometry created along with the hub and the shroud definition was imported into a gridding tool called AutoGrid5 [11]. The blade geometry is the rotor 3 blade of the 3 stage booster from the first part of this 2 part paper. The blade model thus imported is given a tip clearance and other necessary input details like the rotational speed and type of turbomachinery system. The grid generated is medium type with 858149 grid points. The flow path is generated and blade to blade meshes are created as shown in Figure 16.

### CFD solver: Euranus

Euranus, the Fine/Turbo solver is run with inlet boundary conditions of absolute total pressure, absolute total temperature, spanwise distribution of  $\alpha_x$  at inlet and  $\phi$  coming from the previous blade row and static pressure as the exit boundary condition. An isolated blade row 3D CFD analysis of rotor 3 of the booster optimum shown as point 1 in Part 1 of this paper has been performed. Because of the thick boundary layer of the axisymmetric analysis, the first displaced streamline was used to define the hub and the last displaced streamline was used to define the casing. The simulation resulted in an adiabatic efficiency of 91.25%. This compares 93.47% from the T-Axi axisymmetric code loss model [5]. Several runs were done on this case by

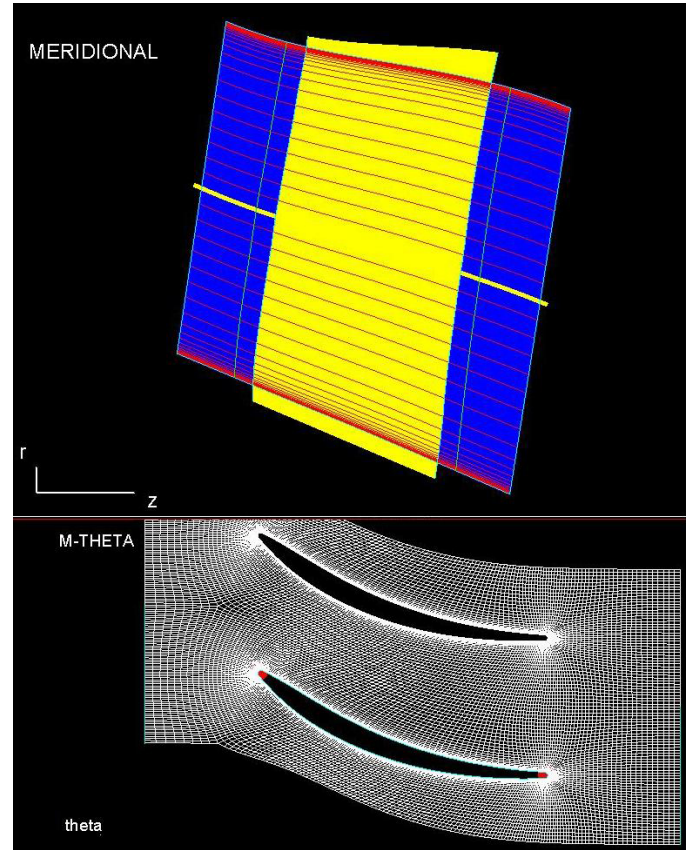


Figure 16. Creating the meridional and blade to blade mesh.

varying the back pressure to match the design mass flow rate of 92.229 kg/s. Figure 17 shows the mass flow rate variation with the total pressure ratio and Figure 18 shows the variation of mass flow rate with the isentropic efficiency and the wide range of the mass flow rate for the booster can be noticed. Figure 19 shows the contour plot of relative mach numbers from 0.2 to 0.8 on three constant radius cut-planes across rotor 3 of the booster. It also shows stream ribbons across the tip clearance showing the tip vortex. Reasonable agreement between the axisymmetric and 3D demonstrates how the coupled system can be used for optimizing a design.

The isolated blade row 3D CFD analysis of rotor 3 of the booster optimum shown as point 2 in Part 1 of this paper was also performed which resulted in corner separation at the exit with an adiabatic efficiency of 93.17%. The lean of the 3D blade geometry was modified as shown in Figure 20 which eliminated the separation near the exit as shown in Figure 21 which is the comparison of the iso surface of axial velocity for the original and modified rotor 3 for this case. The adiabatic efficiency increased to 93.93%. This compares to the T-Axi efficiency of 95.27% for this rotor. It should be noted that this is still not an optimum. The shape shows that there might be stress issues except that the wheel speed is so low and that is why the coupling with a finite element structural solver is so important.

Also, an isolated blade row 3D CFD analysis of stator 4 of the booster optimum shown as point 1 and of stator 4 of the booster optimum shown as point 2 in part 1 of this paper were performed. The loss coefficient,  $\bar{\omega}$  for stator 4 of point 1 is 0.0816

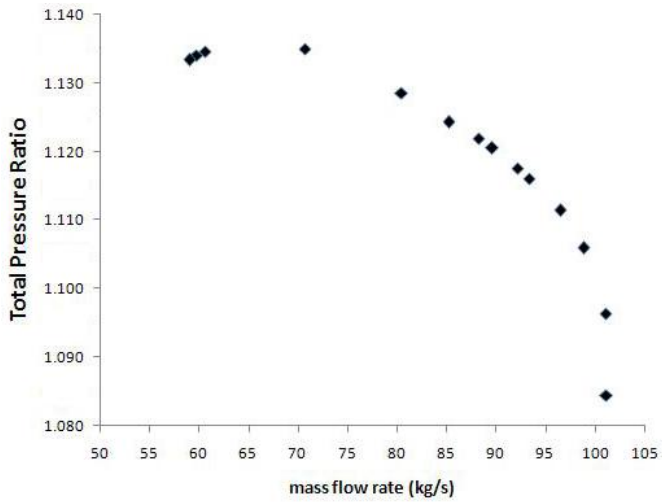


Figure 17. Characteristic curve showing Total PR vs mass flow rate.

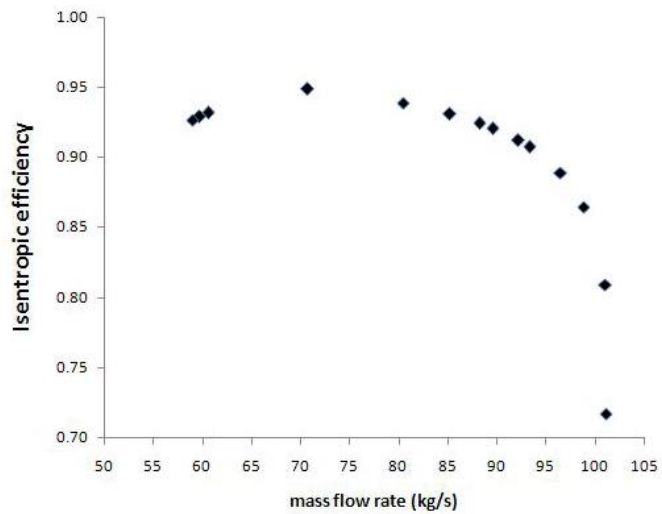


Figure 18. Characteristic curve showing Isentropic efficiency vs mass flow rate.

compared to 0.0497 obtained from the T-Axi axisymmetric code loss model [5] and for stator 4 of point 2 is 0.0817 compared to 0.0376 obtained from T-Axi. These differences and the rotor efficiency differences are due to the fact that the 3D blade geometry obtained is not the optimum blade geometry compared to the T-axi optimized result and T-Axi assumes a perfect execution of the process. The T-Axi loss may also be optimistic for these blades. Better match of the loss coefficient values can be expected when the 3D blade geometry parameters are tied to an optimizer.

### STRUCTURAL ANALYSIS OF BOTH BLADE AND DISK

A Disk is defined parametrically by T-Axi Disk [12] and a 3D model of the disk is generated using UG-NX(CAD package). Structural Analysis is performed on both the disk and the blade generated using ANSYS V12.0. A web disk shape is demonstrated since this is more involved than the ring disks used in the booster design.

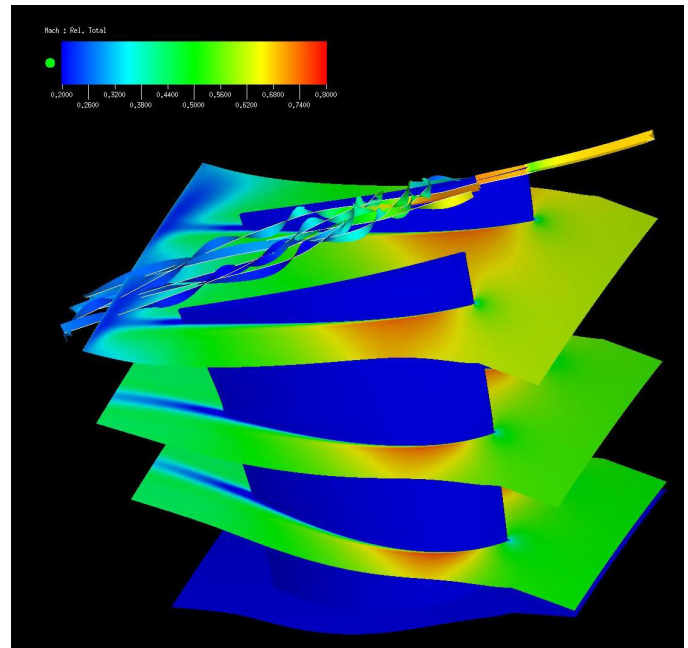


Figure 19. Relative Mach contours of rotor 3 of the optimized booster with stream ribbons at over the tip clearance.

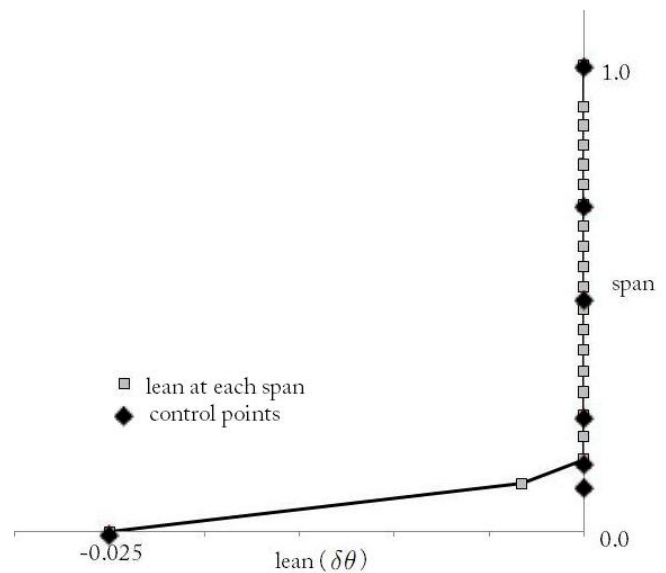


Figure 20. Spanwise lean modification on rotor 3.

### Disk Analysis

An automated script (ANSYS.ain) is used as the input for the structural analysis of the disk. The script file contains all the details about the geometrical and material properties of the disk. Once the file is opened in ANSYS a meshed disk appears as shown in the Figure 22. It is a hexagonal mesh with 166800 nodes and 149650 elements. A modal analysis is performed with 5 modes and the procedure is as follows:

Analysis type is defined.

**Solution** → **Analysis Type** → **New Analysis** → **Modal**.

Analysis option is set.

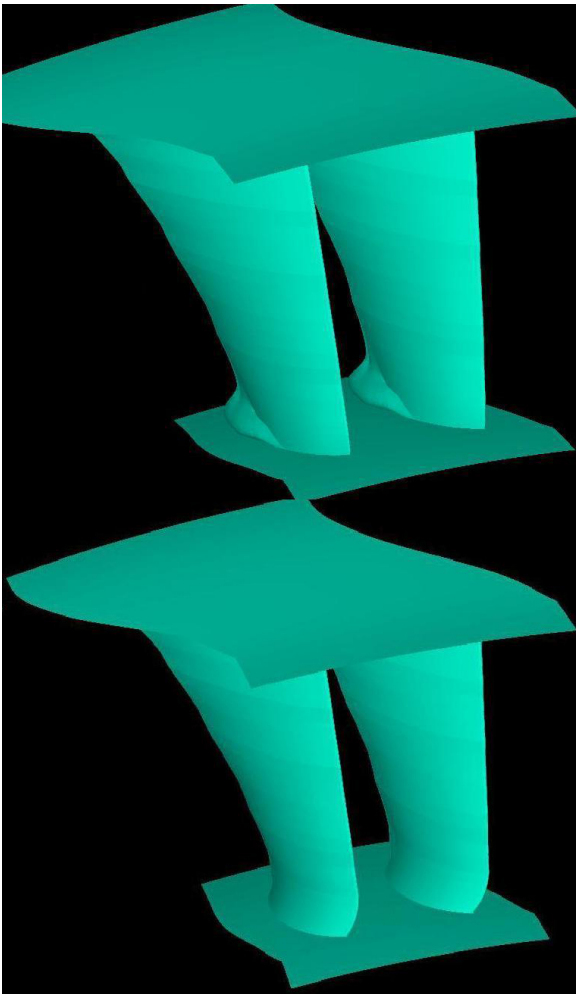


Figure 21. Iso surface comparison of axial velocity for original and modified rotor 3 of the booster optimum point 2.

**Solution** → **Analysis Type** → **Analysis Options** → **PCG Lanczos**.

Number of modes to extract is 5 and it extracts modes for all DOF's.

Constraints are applied.

**Solution** → **Define Loads** → **Apply** → **Structural** → **Displacement** → **On Areas**.

The inner area at the bore of the disk is selected as shown in figure 23.

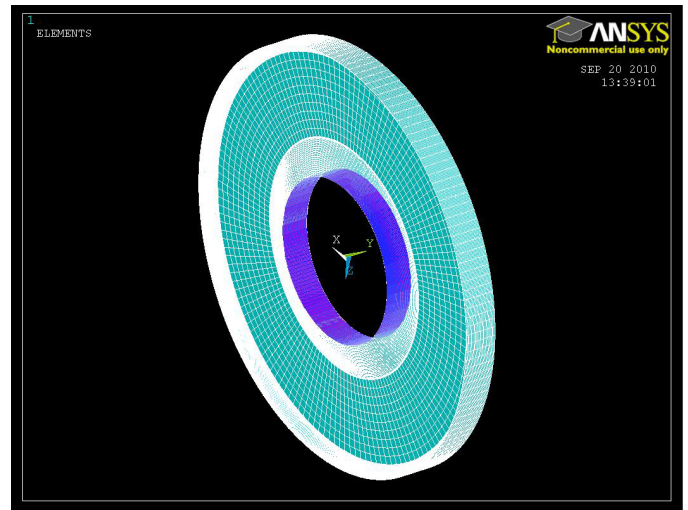


Figure 23. Area to be constrained on the Disk

The system is solved.

**Solution** → **Solve** → **Current LS**.

After the solution is complete, post processing is performed. Figure 24 shows the contour plots of the Displacement vector sum of DOF solution under Nodal solution for all the 5 modes of the disk. The plots are of a deformed shape of the disk.

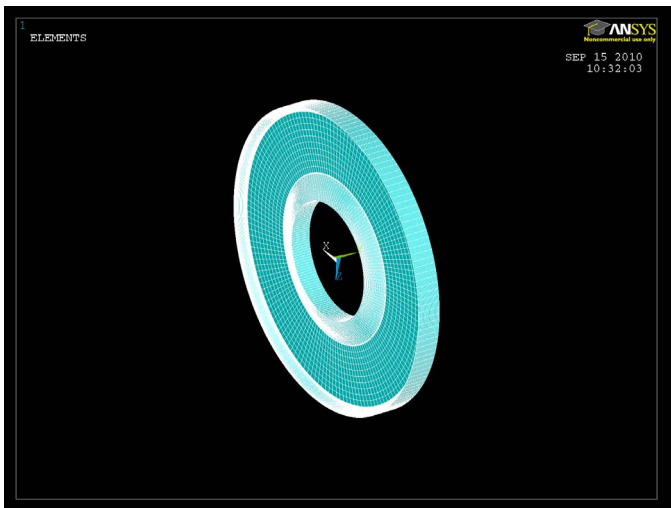


Figure 22. 8 (hexahedron) node 185 brick element type disk is meshed in ANSYS V12.0.

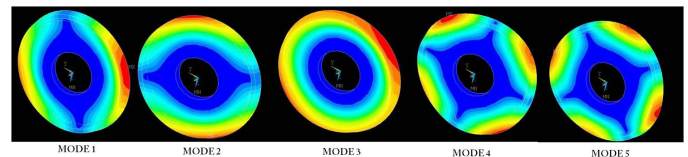


Figure 24. Contour plots of displacement vector sum for all the modes of a disk under Nodal solution.

Also, Figure 25 shows the deformed disk due to the displacement caused near the rim of the disk. This completes the structural modal analysis of a disk.

### Blade Analysis

The blade model used for the structural analysis is the rotor 1 blade of the GE EEE High Pressure Compressor. A part file of the 3D blade model is imported and a script file called 'Blade.ain'

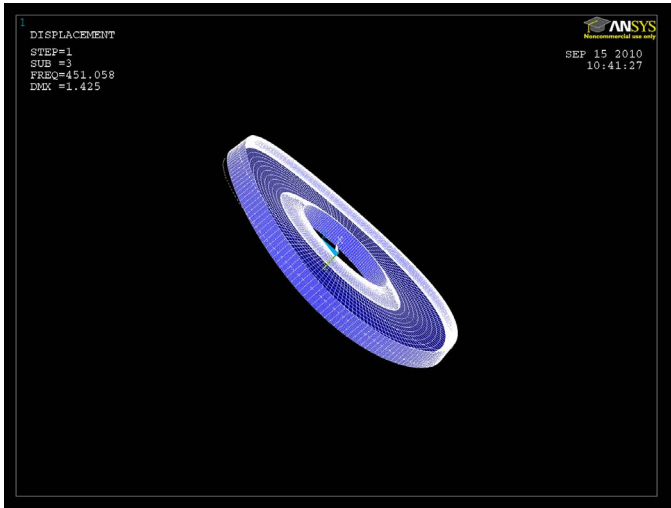


Figure 25. Deformed disk.

is loaded which contains the material properties of the blade and instructions for meshing the blade. This creates a meshed blade with hexagonal mesh, 2093 nodes and 1152 elements as shown in Figure 26 and is ready for structural analysis. A modal analysis

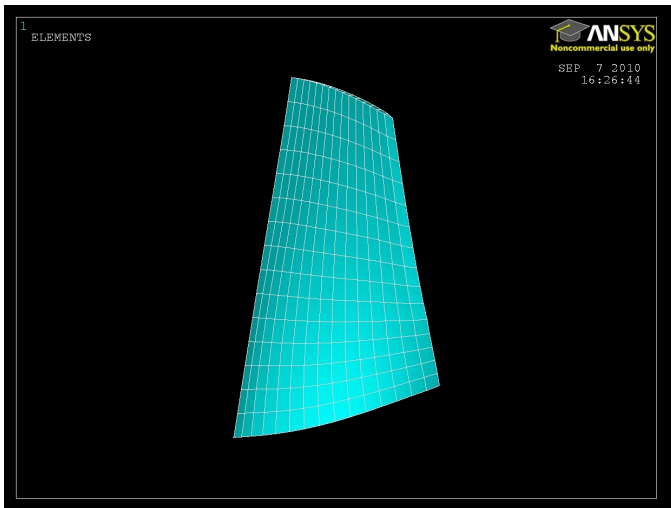


Figure 26. 8 (hexahedron) node 185 brick element type blade is meshed in ANSYS V12.0.

is performed with 14 modes and the procedure is as follows:

Analysis type is defined.

**Solution** → **Analysis Type** → **New Analysis** → **Modal**.

Analysis option is set.

**Solution** → **Analysis Type** → **Analysis Options** → **PCG Lanczos**.

Number of modes to extract is 14 and it extracts modes for all DOF's.

Constraints are applied.

**Solution** → **Define Loads** → **Apply** → **Structural** → **Displacement** → **On Areas**.

The hub area of the blade is selected.

The system is solved.

**Solution** → **Solve** → **Current LS** .

After the solution is complete post processing is performed. Figure 27 and Figure 28 shows the contour plots of the Displacement vector sum of DOF solution under Nodal solution for all the 14 modes of the blade. The plots are of a deformed shape of the blade.

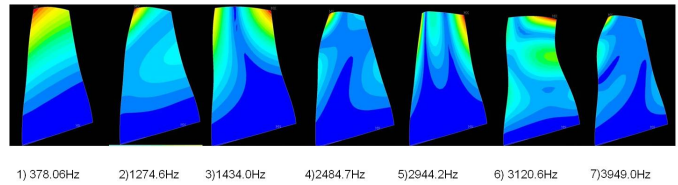


Figure 27. Contour plots of displacement vector sum for first 7 modes of a blade under Nodal solution.

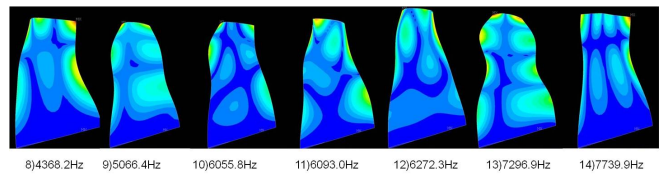


Figure 28. Contour plots of displacement vector sum for last 7 modes of a blade under Nodal solution.

Also, Figure 29 shows the displaced blade with the undisplaced blade shape keeping the hub of the blade fixed. This completes the structural analysis of the blade.

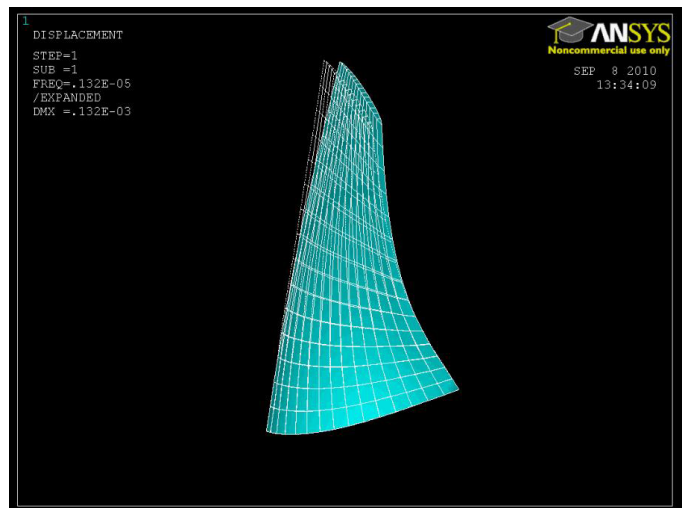


Figure 29. Displaced blade.

## HIGH-FIDELITY OPTIMIZATION

A groundwork for parameterization and automation is done as explained in this paper and it can be then tied to an optimizer. A high-fidelity optimization of the parameters involved in creating the blade geometry can be done with single or multi-objective functions. Chosen parameters from the parameter set can be optimized with specified constraints to obtain an optimized design using optimization software like Dakota [13].

## 3-STAGE BOOSTER DESIGN

Optimization of a 3-stage booster flow path geometry along with the blades was performed and the best result was used as the input for building 3D blades for this design. After generating all the blades, the assemblies were created using Unigraphics-NX(CAD package). Figure 30 shows the 3D model of the rotor assembly of the booster with the wide blade as the fan blade. Figure 31 shows the complete booster assembly showing the split casing with stators and rotors with the fan blade. The hub and casing are the surface of revolution of the hub and casing definition obtained by the optimized flowpath of the booster.

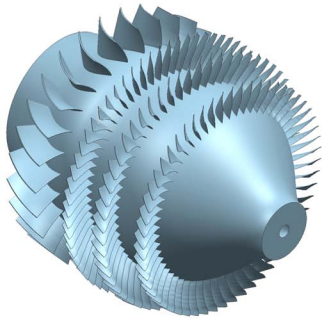


Figure 30. 3-Stage Booster rotor assembly with the Fan blades.

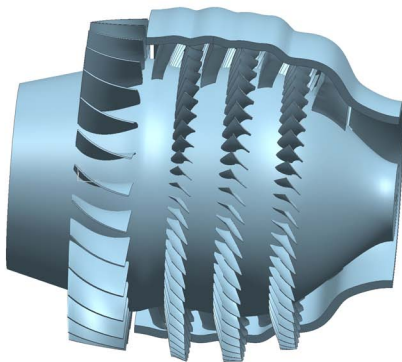


Figure 31. 3-Stage Booster assembly with the split casing.

## CONCLUSIONS & FUTURE WORK

A parametric approach of the blade geometry modeling tool for turbomachinery system has been presented. The benefits of this new method are a large design space including many stacking options with a small number of parameters. The geometry thus obtained was coupled with a CFD solver and a finite element solver was demonstrated which determines the stresses and the mode shapes. An initial 3D representation has been made of the 3 stage booster plus fan hub presented in part 1 of this 2 part paper. A 3-Stage Booster was designed using this tool. The flexibility of the geometry tool has been demonstrated by locally modifying the lean in the hub to eliminate a corner separation. The geometry tool and the demonstrated connection of this tool to a CFD code and FEA code is part of a complete high fidelity design system.

Future work will focus on defining the camber line parametrically and dealing with hot and cold shapes of the blade geometry taking the incidence and deviation angles into consideration. The CFD and FEA are nearly automated, but this must be demonstrated, and the system tied to an optimizer.

## ACKNOWLEDGMENT

The authors would like to thank NASA for funding and support through NRA NNC07CB61C - "MDAO of Turbomachinery with Emphasis on Component Optimization".

## REFERENCES

- [1] Gräsel, J., Keskin, A., Swoboda, M., Przewozny, H., and Saxer, A., 2004. "A full parametric model for turbomachinery blade design and optimisation". DETC Paper Number DETC2004-57467.
- [2] Dutta, A. K., Flassig, P. M., and bestle, D., 2008. "A non-dimensional quasi-3d blade design approach with respect to aerodynamic criteria". ASME Paper Number GT2008-50687.
- [3] Turner, M. G., Park, K., Siddappaji, K., Dey, S., Gutzwiller, D. P., Merchant, A., and Bruna, D., 2010. "Framework for multidisciplinary optimization of turbomachinery". ASME Paper Number GT2010-22228.
- [4] University of Cincinnati T-Axi Website <http://gtsl.ase.uc.edu/T-AXI/>.
- [5] Turner, M. G., Merchant, A., and Bruna, D., 2006. "A turbomachinery design tool for teaching design concepts for axial-flow fans, compressors, and turbines". ASME Paper Number GT2006-90105.
- [6] Turner, M. G., Bruna, D., and Merchant, A., 2007. "Applications of a turbomachinery design tool for compressors and turbines". AIAA Paper Number 2007-5152.
- [7] Bruna, D., Cravero, C., Turner, M. G., and Merchant, A., 2007. "An educational software suite for teaching design strategies for multistage axial flow compressors". ASME Paper Number GT2007-27160.
- [8] Haimes, R., and Follen, G. J., 1998. "Computational analysis programming interface".
- [9] Merchant, A., and Haimes, R., 2003. "A cad-based blade geometry model for turbomachinery aero design systems". In GT-2003-38305.

- [10] NUMECA International. FINE/Turbo  
<http://numeca.be/index.php?id=16>.
- [11] NUMECA International. Autogrid  
<http://numeca.be/index.php?id=25>.
- [12] Gutzwiller, D. P., Turner, M. G., and Downing, M. J., 2009.  
“Educational software for blade and disk design”. ASME  
Paper Number GT2009-59692.
- [13] Sandia National Laboratories - DAKOTA Website  
<http://www.cs.sandia.gov/DAKOTA/>.